ELSEVIER

Ceramics International 33 (2007) 187–192

CERAMICS INTERNATIONAL

www.elsevier.com/locate/ceramint

# Dependence of the nonlinear electrical behavior of $SnO_2$-based varistors on $Cr_2O_3$ addition

F.M. Filho [a], A.Z. Simões [a,*], A. Ries [a], L. Perazolli [a], E. Longo [b], J.A. Varela [a]

[a] *Chemistry Institute, Department of Chemistry-Physics, UNESP C.P. 355, CEP 14801-970 Araraquara-SP, Brazil*
[b] *Chemistry Department, Universidade Federal de São Carlos, UFSCar-São Carlos, SP, CEP-13565-905, Brazil*

Received 22 March 2005; received in revised form 6 June 2005; accepted 5 July 2005
Available online 28 November 2005

**Abstract**

Tin dioxide varistors doped with CoO, ZnO, $Ta_2O_5$ and $Cr_2O_3$ were prepared by the mixed oxide method. Temperature dependent impedance spectroscopy revealed two different activation energies, one at low frequencies and the other at high frequencies. These activation energies were associated with the adsorption and reaction of $O_2$ species at the grain boundary interface. We show that $Cr_2O_3$ improves the varistor properties, generating sites for the adsorption of $O'$ and $O''$ at the grain boundary region. The $O'$ and $O''$ defects are truly responsible for the barrier formation at the grain boundary interface.


*Keywords:* E. Varistors; Tin dioxide; Impedance spectroscopy

## 1. Introduction

$SnO_2$ has a tetragonal structure, similar to the rutile structure, and behaves as an n-type semiconductor [1]. This oxide has been extensively described in the literature because of its importance as a gas and humidity sensor [2–4]. These properties, along with electrical ones, are dependent on the nonstoichiometry surface produced by powder preparation, thermal treatment and atmosphere present in the oven during the preparation of the material [2–4]. High densification can be achieved by the addition of CoO, $MnO_2$, or even ZnO to $SnO_2$, allowing for nonohmic properties [5–7]. The nature of the potential barrier was characterized in $SnO_2$-based varistor systems and found to be Schottky-like, similar to that frequently reported for the traditional ZnO-based varistor system, despite the fact that $SnO_2$-based varistors differ microstructurally from the ZnO-based varistor [8].

The addition of $Ta_2O_5$ creates $Ta_{Sn}^{\bullet}$ defects (donor) that increase the lattice conductivity of $SnO_2$-based ceramics [9]. Moreover, in small concentrations $Ta_2O_5$ does not segregate at the grain boundaries resulting in a high grain conductivity. Excess of $Ta_2O_5$ causes segregation of defects at grain boundaries which decrease both, bulk conductivity and grain size. Bueno et al. reported that the varistors of $(98.95 - x)\%$ $SnO_2 + 1.0\%$ $CoO + 0.05\%$ $Nb_2O_5 + x\%$ $Cr_2O_3$ sintered at 1300 °C for 1 h would lose their nonlinearity when $x = 0.05$ in molar system due to the possibility of $CoCr_2O_4$ formation at the grain boundaries [10]. The nonohmic electrical behavior of traditional ZnO and $SrTiO_3$-based ceramics, as discussed in Refs. [11] and [12], is linked to oxygen, which plays a key role in the grain boundaries of such ceramics. An absorbed layer of bismuth with a thickness of about ≈5 Å in a ZnO-based varistor is necessary to create potential barriers at the grain boundaries, and the height of these potential barriers largely depends on the excess oxygen present at the interface between the grains [11]. However, very little is known about the chemical nature of grain boundary interfaces in metal oxide varistors and its relationship to nonohmic electrical behavior. Therefore, the main purpose of this article is to show that the chemical origin of the potential barrier in polycrystalline ceramics depends on the amount of oxygen present at grain boundary interfaces. Furthermore, the main role of transition metal oxide as a dopant is to control the oxygen concentration at the grain boundary interface. Based on this evidence, a chemical barrier formation mechanism is proposed to explain the physical origin of interfacial trapping states.

* Corresponding author. Tel.: +55 16 3301 6600; fax: +55 16 3322 7932.
*E-mail address:* alezipo@yahoo.com (A.Z. Simões).

0272-8842/$32.00 
doi:10.1016/j.ceramint.2005.07.025

## 2. Experimental

The varistors were obtained from the mixed oxide method in alcoholic medium. All the oxides used were analytical grade: $SnO_2$ (Cesbras-Fine), ZnO (Synth) CoO (Riedel), $Ta_2O_5$ (Aldrich), $Cr_2O_3$ (Vetec). The molar composition of the investigated systems was $(98.95 - X)\%$ $SnO_2 + 0.50\%$ CoO + 0.50% ZnO + 0.05% $Ta_2O_5 + X\%$ $Cr_2O_3$, with $X$ equal to 0 or 0.050 mol%. The amounts of CoO and ZnO were always kept constant, because these additives were used to facilitate densification during sintering. The powder was pressed into pellets by uniaxial pressing followed by isostatic pressing at 210 MPa. The pellets were sintered at 1400 °C for 2 h in oxygen atmosphere and slowly cooled to room temperature (5 °C $min^{-1}$). The X-ray data were collected with a Rigaku-2000 diffractometer under the following experimental conditions: copper anode, 50 kV, 150 mA, Cu Kα radiation monochromatized by a graphite crystal. The tetragonal structure (rutile structure) of the $SnO_2$ starting material was confirmed by X-ray diffraction. Mean grain size was determined by analyzing the SEM micrographs (Topcom Sm-300). To perform the electrical measurements, silver contacts were deposited on the sample surfaces. Current-tension measurements were taken using the High Voltage Measure Unit (Keithley Model 237). The electric breakdown field ($E_b$) was obtained at a current density of 1 mA $cm^{-2}$. The impedance measurements were made with a frequency response analyser (HP4194A) using frequency ranging from 5 Hz up to 13 MHz, with an amplitude voltage of 1 V. The pellets were put in a sample holder inserted to a furnace. Measurements of the real ($Z'$) and the imaginary plot of the impedance ($Z''$) were made at temperatures ranging from 100 to 400 °C. The impedance data were analyzed with the EQUIVCRT program [13].

## 3. Results and discussion

Fig. 1 shows the X-ray diffraction analysis of a $SnO_2$-based varistor system with a molar concentration of 0.50% CoO + 0.50% ZnO + 0.05% $Ta_2O_5$ and 0.50% CoO + 0.50% ZnO + 0.05% $Ta_2O_5$ + 0.05% $Cr_2O_3$. Besides the $SnO_2$ rutile phase, no secondary phase was observed. A sintering study combined with XRD results indicated that sintering at 1400 °C for 2 h are the optimal conditions to obtain crystalline, dense $Cr_2O_3$*$Ta_2O_5$*CoO*ZnO-doped $SnO_2$ varistors containing only the expected rutile phase. The amount of additives is very small and other possible phase might not be detected because of the detection limit of the XRD equipment. All dopants introduced in the $SnO_2$ matrix lead to a stable solid solution according to the Eqs. (1)–(5).

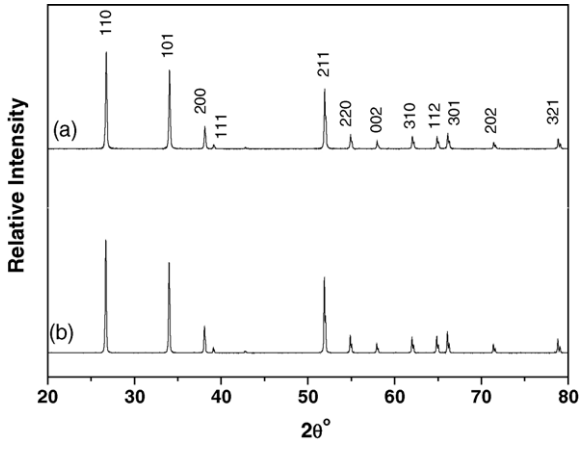


Fig. 1. X-ray diffraction data of the varistor system doped with chromium concentrations: (a) without Cr; (b) 0.050 mol%.

$$ZnO \xrightarrow{SnO_2} Zn''_{Sn} + V_0^{\bullet\bullet} + O_O^x \quad (1)$$

$$CoO \xrightarrow{SnO_2} Co''_{Sn} + V_0^{\bullet\bullet} + O_O^x \quad (2)$$

$$Co_2O_3 \xrightarrow{SnO_2} 2Co''_{Sn} + V_0^{\bullet\bullet} + 2O_O^x \quad (3)$$

$$V_0^{\bullet\bullet} + Ta_2O_5 \xrightarrow{SnO_2} 2Ta_{Sn}^{\bullet} + 5O_O^x \quad (4)$$

$$Cr_2O_3 \xrightarrow{SnO_2} 2Cr'_{Sn} + V_0^{\bullet\bullet} + 3O_O^x \quad (5)$$

Fig. 2 shows the SEM micrographs of two systems considered in this study. Considering the $SnO_2$ varistor microstructure a Schottky-type electrical barrier can be ascribed to be most likely barrier at the $SnO_2$ grain boundary, since no intergranular insulating layer separating two $SnO_2$ grains was observed. The negative surface charge at the grain boundary interface is compensated by the positive charge in the depletion layer in the grain on both sides of the interface [8,14,15]. However, electron dispersive spectroscopy revealed that there is no difference in dopant concentration between grain and grain boundary. The densities of sintered samples were obtained by the Arquimedes method and are related to the theoretical density of $SnO_2$ ($\rho_{theoretical} = 6.95$ g $cm^{-3}$). The final densities after sintering are higher than 98%, as shown in Table 1. They were only slightly affected by $Cr_2O_3$ addition, although the average grain size decreased significantly with the $Cr_2O_3$ addition. The $SnO_2$ ceramic densification has been mainly attributed to the effect of dopants substitution in the SnO matrix which leads to the formation of oxygen vacancies, providing the increase of the diffusion coefficient of ions, and thus, promoting the sintering.

Cerri et al. found relative density above 99%, showing that CoO is extremely active in the promotion of the $SnO_2$ densification, even with low concentration of dopants. They attributed the high densification to the increased concentration of oxygen vacancies in the grain boundary region. They proposed reaction (1) for the formation of oxygen vacancies when $SnO_2$ is doped with CoO. These results are in agreement with the work of Yuan et al., who demonstrated that the $Li^+$ ion also promotes $SnO_2$ densification by increasing the flux of

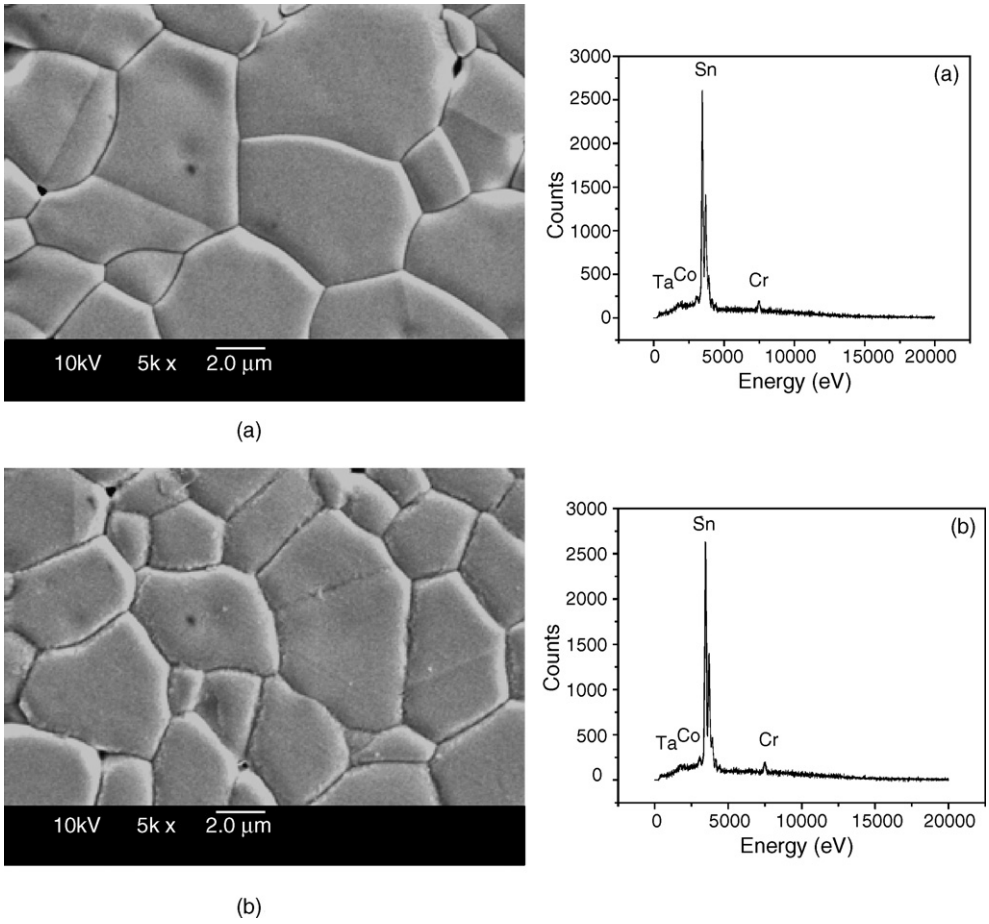


Fig. 2. SEM micrographs together with electron dispersive spectroscopy results for the SZCT system doped with chromium concentrations: (a) without Cr; (b) 0.05 mol%.

species that diffuse inside the material. Pianaro et al. observed that when the basic $SnO_2$ varistor is doped with $Cr_2O_3$ the grain size decreased, indicating that $Cr_2O_3$ inhibits grain growth during sintering [16,17].

Fig. 3a illustrates the response of impedance spectroscopy at 300 °C for two systems considered in this study. From a previous paper the best nonlinear electrical properties were observed for samples doped with 0.05 mol% $Cr_2O_3$ [18]. Therefore, this composition was chosen to evaluate the phenomena involved on the electrical properties of the varistor system. It can be noted that the grain boundary resistance increases with the addition of chromium dioxide. All the semicircular arcs in the complex plane in Fig. 3 yield to an arc, with the center displaced below the real axis, due to the presence of distributed elements and a relaxation process resulting from the trapped states. Table 1 presents the $\phi_b$ (barrier height) values, calculated, as suggested in Ref. [3], for a back-to-back Schottky-type potential barrier of $SnO_2$ and CoO-

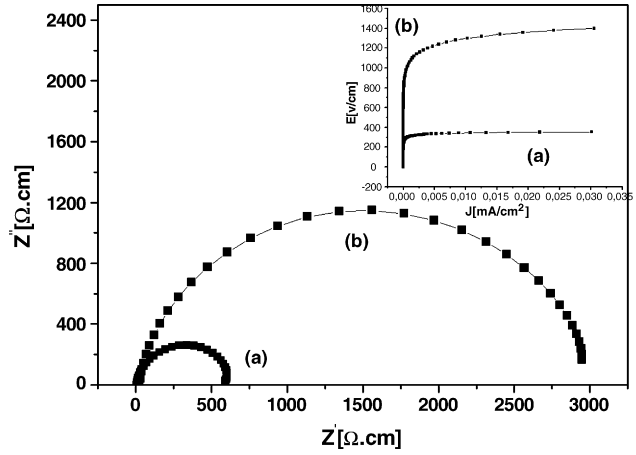


Fig. 3. Nyquist diagram obtained at 300 °C for SZCT system doped with chromium concentrations: (a) without Cr; (b) 0.05 mol%. Inset of applied electric field as a function of current density for the SZCT system doped with chromium concentrations: (a) without Cr; (b) 0.05 mol%.

Table 1
Influence of the $Cr_2O_3$ on the relative densities, grain sizes, nonlinear coefficients ($\alpha$) and breakdown fields ($E_b$) for the SZCT system

| $SnO_2$ | CoO | ZnO | $Ta_2O_5$ | $Cr_2O_3$ | $\rho_r$ (%) | $\phi_b$ eV | ($\alpha$) | $E_b$ (V cm$^{-1}$) | $V_b$ (V/barrier) | Grain size (µm) ±1% |
|---|---|---|---|---|---|---|---|---|---|---|
| 98.95 | 0.5 | 0.5 | 0.05 | – | 98.5 | 0.70 | 11.5 | 1100 | 1.49 | 13.5 |
| 98.90 | 0.5 | 0.5 | 0.05 | 0.050 | 98.5 | 0.95 | 20.4 | 3050 | 2.41 | 7.9 |

based varistor systems. Based on these values, it can be concluded that the addition of $Cr_2O_3$ causes a significant increase in the barrier height.

The increase in the potential barrier height and in the barrier width are associated to the increase of both negative states at the interface between the $SnO_2$ grain (Ns) and donor concentration (Nd) due to the segregation of $Cr_2O_3$ next to grain boundary as well as the creation of positive defects in the depletion layer ($V_0^{\bullet\bullet}$) and negative defects interface ($Cr'_{Sn}$) [19–21].

This suggests that the electronic states of the grain boundary region change with the addition of $Cr_2O_3$. The applied electric field as a function of current density for the different systems is given as an inset in Fig. 3b. The nonlinear coefficient $\alpha$ was obtained by $\alpha = \log(I_2/I_1)/(V_2/V_1)$ where $V_1$ and $I_1$ as well as $V_2$ and $I_2$ are corresponding values of voltage and current for two points that can be chosen arbitrarily [22]. The $\alpha$ values were obtained from the curves ExJ for current densities between 1 and 10 mA $cm^{-2}$. It was observed that the addition of $Cr_2O_3$ leads to a substantial modification in the electrical behavior of the $SnO_2$*ZnO*CoO*$Ta_2O_5$ ceramics. The $Cr_2O_3$ free system, although nonlinear, is highly resistive. The samples containing 0.05 mol% $Cr_2O_3$ are more resistive (electrical breakdown close to 3050 V $cm^{-1}$) and possess a nonlinear coefficient equal to 20.4. This occurs because the electron concentration decreases in the specimen with $Cr_2O_3$. Comparing the results presented in Table 1 and Fig. 3, it can be concluded that the addition of $Cr_2O_3$ decreases the grain size increasing the nonlinear coefficient and the electric breakdown field. Similar results were found by Bueno et al. [8] where they described the DC electrical behavior of the SCN system as a function of different $Cr_2O_3$ molar concentrations. The authors observed that the SCN presents a varistor behavior with $\alpha$ equal to 58 and an electric breakdown field ($E_b$) of 1870 V $cm^{-1}$. When 0.05 mol% $Cr_2O_3$ was added to the system, the $\alpha$ value increased to 41 and the breakdown field to 3990 V $cm^{-1}$.

Fig. 4 presents the Bode diagrams for the SZCT and SZCTCr systems at 300 °C. When 0.05 mol% $Cr_2O_3$ is added to SZCT an increase in the system resistivity is observed for both, the high and low frequencies time constant. These resistivity differences decrease as the temperature is increased, thus indicating a higher activation energy for the SZCTCr system when compared to SZCT (not shown in the article).

Fig. 5 presents the high and low frequency (1 MHz and 1 KHz, respectively) and region capacitances as a function of the temperature for all of the investigated samples. In Fig. 5, the capacitance for SZCTCr system is higher when compared to SZCT, which is probably associated with the decrease in the grain boundary barrier width. The addition of $Ta_2O_5$ creates $Ta_{Sn}^{\bullet}$ defects (donor) which form a solid solution with $SnO_2$ and lead to an improved grain boundary conductivity. The importance of CoO defects is the creation of oxygen vacancies in the grain boundary region, which is fundamental for the sintering process [23]. On the other hand, the presence of $Cr'_{Sn}$ and $Co''_{Sn}$ leads to barrier formation in the grain boundary region. The defects generated by these two dopants are necessary for a varistor system. However, building up a high and narrow potential barrier at the grain boundary is the last condition required for obtaining a varistor with a high nonlinear coefficient. The obtained data show that doping the SZCT system with $Cr_2O_3$ at a level of 0.05 mol% builds up an optimized barrier at the grain boundary. Kim et al. [24] observed that the activation energies for the O′ and O″ species on the $SnO_2$ surface are 0.6 and 1.0 eV, respectively. The corresponding energies in the present article are 0.446 and

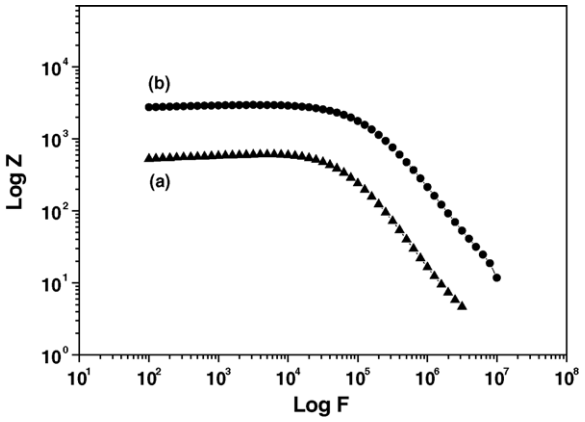


Fig. 4. Impedance as function of frequency logarithm (Bode diagrams) for SZCT system sintered at 1400 °C for 2 h and doped with chromium concentrations: (a) without Cr; (b) 0.05 mol%.

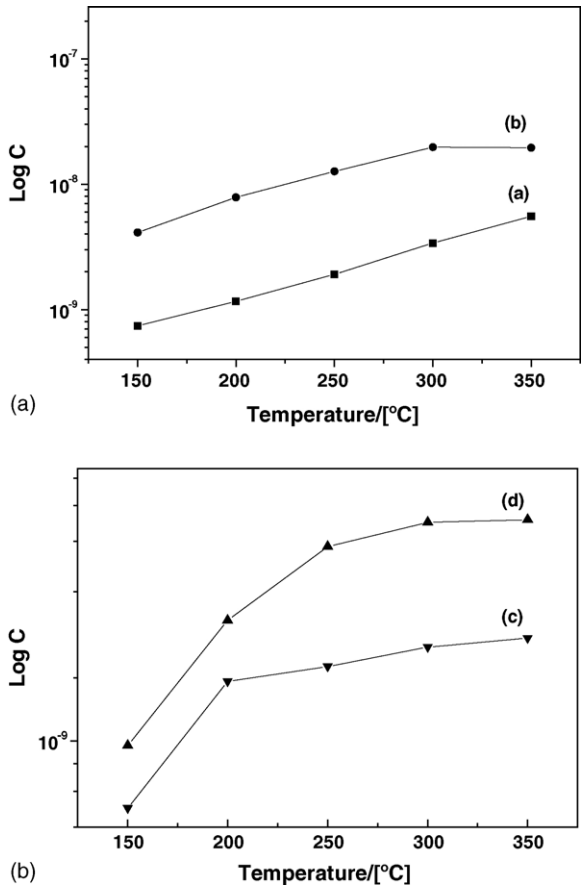


Fig. 5. Capacitance as a temperature function for (a) high and (b) low frequency regions for SZCT system sintered at 1400 °C 2 h and doped with chromium concentrations: (a) without Cr; (b) 0.05 mol%; (c) without Cr; (d) 0.05 mol%.

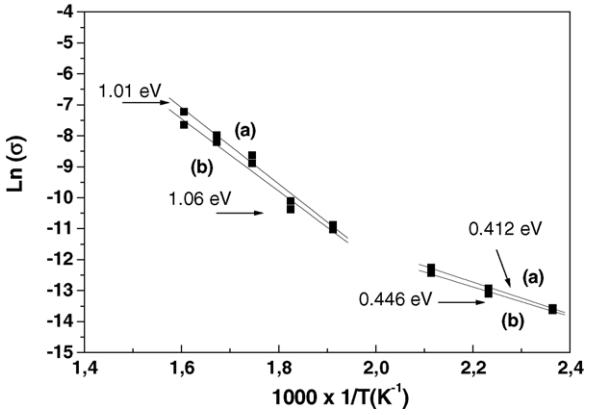


Fig. 6. Activation energies calculated from the Arrhenius plot for the high (a) and (b) low frequency regions for the temperature range lower and higher than 200 °C (SZCT system sintered at 1400 °C 2 h and doped with 0.05 mol% chromium).

1.06 eV for the SZCTCr compounds at temperatures higher than 200 °C (low frequency) and 0.412 and 1.01 at temperatures lower than 200 °C (high frequency—Fig. 6). It is possible that these species predominate at the grain boundary structure and their formation can be represented by the following reactions:

$$Cr'_{Sn} + O_2 \xrightarrow{SnO_2} Cr'_{Sn}O_{2(ads)} \quad (6)$$

$$Cr'_{Sn}O_{2(ads)} \xrightarrow{SnO_2} Cr^{x}_{Sn}O'_{2(ads)} \quad (7)$$

$$Cr^{x}_{Sn}O'_{2(ads)} + Cr'_{Sn} \xrightarrow{SnO_2} (Cr^{x}_{Sn})_2O''_{2(ads)} \quad (8)$$

$$Cr'_{Sn}O''_{2(ads)} + O_2 + Cr'_{Sn} \xrightarrow{SnO_2} 2(Cr^{x}_{Sn}O'_{2(ads)}) \quad (9)$$

$$Cr^{x}_{Sn}O'_{2(ads)} + Cr'_{Sn} \xrightarrow{SnO_2} (Cr^{x}_{Sn})_2O''_{(structural)} \quad (10)$$

The adsorbed oxygen at the grain boundary captures electrons from negatively charged defects at the grain boundary and stays at the interface. This effect was confirmed by impedance analysis [25].

The role of $Cr'_{Sn}$ is to increase the O′ and O″ adsorption at the grain boundary interface and to promote a decrease in the conductivity by donating electrons to $O_2$ adsorbed at the grain boundary. From these results one may gather that the species that are truly responsible for the barrier formation are O′ and O″. The $Cr'_{Sn}$ generates the sites to promote the adsorption of electrophilic species. These defects, O′ and O″, are not equally present at the same grain boundary. A random distribution of the O′ and O″ defects would lead to different charge transport paths in the samples.

Electron energy loss spectroscopy (ELS) results suggest that adsorbed $O'_2$ formation requires oxygen vacancy sites of $TiO_2$, although the vacancies need not be directly involved in binding the $O'_2$ species [26]. To the best of our knowledge, five theoretical studies have recently found (O′ and O″) and $SnO_2$ species at the surface.

On the other hand, oxygen vacancies and electronic states on $SnO_2$ surface, are related to each and have been exhaustively studied [27–30]. Oxygen also plays a key role in the grain boundaries of ZnO or $SrTiO_3$ varistors, since it indicates that the chemistry of boundaries determines the nonohmic behavior [31,32].

## 4. Conclusions

In summary, different kinds of defects in the grain boundary region were observed in our varistor system. A change in the activation energy at 200 °C was attributed to the desorption of species previously adsorbed at the grain boundary. Below this temperature one can observe low activation energy defects which may be related to oxygen vacancies. The presence of $Cr_2O_3$ up to levels of 0.05% improves the varistor properties, generating sites for the adsorption of O′ and O″ at the grain boundary region. The role of $Cr'_{Sn}$ is to create sites promoting the formation of O′ and O″ defects, which are truly responsible for the barrier formation at the grain boundary interface.

## Acknowledgments

The authors gratefully acknowledge the financial support of the Brazilian agencies FAPESP, CNPq, and CAPES and of the German Academic Exchange Service (DAAD).

## References

[1] Z.M. Jarzebski, J.P. Marton, J. Electrochem. Soc. 123 (1976) 199.
[2] S. Semanski, T.B. Fryberger, Sens. Actuat. B 1 (1990) 97.
[3] J. Maier, W. Gopel, J. Solid State Chem. 72 (1988) 293.
[4] W. Gopel, K.D. Shierbaum, H.D. Wiemhofer, Solid State Ionics 28 (1990) 1631.
[5] J.A. Cerri, E.R. Leite, D. Gouvea, E. Longo, J. Am. Ceram. Soc. 79 (1996) 804.
[6] J.A. Varela, J.A. Cerri, E.R. Leite, E. Longo, M. Shamsuzzoha, R.C. Bradt, Ceram. Int. 25 (1999) 256.
[7] M.S. Castro, C.M. Aldao, J. Eur. Ceram. Soc. 18 (1998) 2233.
[8] P.R. Bueno, M.R. Cassia-Santos, E.R. Leite, E. Longo, J. Bisquert, G. Garcia-Belmonte, F. Fabregat-Santiago, J. Appl. Phys. 88 (2000) 6545.
[9] J.A. Cerri, E.R. Leite, D. Gouvêa, E. Longo, J. Am. Ceram. Soc. 79 (1996) 799.
[10] P.R. Bueno, S.A. Pianaro, E.C. Pereira, E. Longo, J.A. Varela, J. Appl. Phys. 84 (1998) 3700.
[11] F. Stucki, F. Greuter, Appl. Phys. Lett. 57 (1990) 446.
[12] Y. Nakano, N. Ichinose, J. Mater. Res. 5 (1990) 2910.
[13] S.P. Jiang, J.G. Love, S.P.S. Bbadwal, Key Eng. Mater. 125 (1997) 81.
[14] D.M. Radecka, K. Zakrezewska, M. Rekas, Sens. Actuat. B 47 (1998) 194.
[15] T.K. Gupta, J. Am. Ceram. Soc. 73 (1990) 1817.
[16] S.A. Pianaro, P.R. Bueno, P. Olivi, E. Longo, J.A. Varela, J. Sci. Mater. Elect. 9 (1998) 159.
[17] S.A. Pianaro, P.R. Bueno, E. Longo, J.A. Varela, Ceram. Inter. 25 (1991) 1.
[18] F.M. Filho, A.Z. Simões, A. Ries, E.C. Souza, L. Perazolli, M. Cilense, E. Longo, J.A. Varela, Ceram. Int. 31 (2005) 399.
[19] A.C. Antunes, S.R.M. Antunes, A.J. Zara, S.A. Pianaro, E. Longo, J.A. Varela, J. Mater. Sci. 37 (2002) 2407.
[20] M. Alim, J. Am. Ceram. Soc. 72 (1989) 32.
[21] K. Mukae, K. Tsuda, I. Nagasawa, J. Appl. Phys. 50 (1979) 4475.

[22] S.C. Chang, J. Vac. Sci. Technol. 17 (1980) 366.
[23] J.C. Fan, J.B. Goodenough, J. Appl. Phys. 48 (1977) 3524.
[24] M.C. Kim, K.H. Song, J. Park, J. Mater. Res. 8 (1993) 1368.
[25] F.M. Filho, A.Z. Simões, A. Ries, L. Perazolli, E. Longo, J.A. Varela, Ceram. Int. 32 (2006) 283–289.
[26] M.A. Henderson, W.S. Epling, C.l. Perkins, C.H.F. Peden, U. Diebold, J. Phys. Chem. B 103 (1998) 5328.
[27] Y. Yamagushi, Y. Naagaswa, A. Murakami, K. Tabata, Int. J. Quant. Chem. 69 (1998) 669.
[28] Y. Yamagushi, Y. Naagaswa, S. Shimomura, K. Tabata, Int. J. Quant. Chem. 74 (1999) 423.
[29] Y. Yamagushi, Y. Naagaswa, S. Shimomura, K. Tabata, E. Suzuki, Chem. Phys. Lett. 316 (2000) 477.
[30] F.R. Seusato, R. Custodio, M. Calatayud, A. Beltran, J. André, J.R. Sanbrano, E. Longo, Surf. Sci. 408 (2002) 511.
[31] F. Stuki, F. Grenter, Appl. Phys. Lett. 57 (1990) 446.
[32] J. Li, S. Li, F. Liu, M.A. Alim, G. Chen, J. Mater. Sci. Mater. Electron. 14 (2003) 483.